Report No. NADC-88007-60

The Microstructural and Phase Characterization of RST A1-Ti-X Alloys

William E. Frazier and James J. Thompson
Air Vehicle and Crew Systems Technology Department
Naval Air Development Center
Warminster, PA 18974

July 1987

Final Report

Prepared for
Airborne Materials Block
Department of the Navy
Warminster, PA 18974-5000

NOTICES

REPORT NUMBERING SYSTEM – The numbering of technical project reports issued by the Naval Air Development Center is arranged for specific identification purposes. Each number consists of the Center acronym, the calendar year in which the number was assigned, the sequence number of the report within the specific calendar year, and the official 2-digit correspondence code of the Command Office or the Functional Department responsible for the report. For example: Report No. NADC-86015-70 indicates the fifteenth Center report for the year 1986 and prepared by the Systems and Software Technology Department. The numerical codes are as follows:

CODE	OFFICE OR DEPARTMENT
00	Commander, Naval Air Development Center
01	Technical Director, Naval Air Development Center
02	Comptroller
05	Computer Department
10	Anti-Submarine Warfare Systems Department
20	Tactical Air Systems Department
30	Warfare Systems Analysis Department
40	Communication & Navigation Technology Department
50	Mission Avionics Technology Department
60	Air Vehicle & Crew Systems Technology Department
70	Systems & Software Technology Department
80	Engineering Support Group

PRODUCT ENDORSEMENT – The discussion or instructions concerning commercial products herein do not constitute an endorsement by the Government nor do they convey or imply the license or right to use such products.

APPROVED BY: W. F. Moroney DATE: Oct 3, 1988

W. F. MORONEY
CAPT, MSC, U.S. NAVY

Unclassified
SECURITY CLASSIFICATION OF THIS PAGE

REPORT DOCUMENTATION PAGE

Form Approved
OMB No 0704-0188

1a REPORT SECURITY CLASSIFICATION Unclassified	1b RESTRICTIVE MARKINGS
2a SECURITY CLASSIFICATION AUTHORITY	3 DISTRIBUTION / AVAILABILITY OF REPORT Approved for Public Release, Distribution is unlimited
2b DECLASSIFICATION / DOWNGRADING SCHEDULE	
4 PERFORMING ORGANIZATION REPORT NUMBER(S) NADC-88007-60	5 MONITORING ORGANIZATION REPORT NUMBER(S)
6a NAME OF PERFORMING ORGANIZATION Naval Air Development Center 6b OFFICE SYMBOL (If applicable) Code 606	7a NAME OF MONITORING ORGANIZATION
6c ADDRESS (City, State, and ZIP Code) Warminster, PA 18974-5000	7b ADDRESS (City, State, and ZIP Code)
8a NAME OF FUNDING / SPONSORING ORGANIZATION Naval Air Development Center 8b OFFICE SYMBOL (If applicable)	9 PROCUREMENT INSTRUMENT IDENTIFICATION NUMBER
8c ADDRESS (City, State, and ZIP Code) Warminster, PA 18974-5000	10 SOURCE OF FUNDING NUMBERS PROGRAM ELEMENT NO: 61153N PROJECT NO: BR2201-01 TASK NO: (P.I.) 4 WORK UNIT ACCESSION NO: ZP180
11 TITLE (Include Security Classification) The Microstructural and Phase Characterization of RST A1-Ti-X Alloys (Unclassified)	
12 PERSONAL AUTHOR(S) William E. Frazier and James J. Thompson	
13a TYPE OF REPORT: Final 13b TIME COVERED: FROM 1 OCT. '87 TO 1 JUL '88	14 DATE OF REPORT (Year, Month, Day): 1 Jul 88 15 PAGE COUNT
16 SUPPLEMENTARY NOTATION	

17 COSATI CODES		
FIELD	GROUP	SUB-GROUP
11	06	
11	06.01	

18 SUBJECT TERMS (Continue on reverse if necessary and identify by block number)
Rapid Solidification, Aluminum, titanium, aluminum alloys, vanadumm, cerium, titanium alloys, rst

19 ABSTRACT (Continue on reverse if necessary and identify by block number)

Powder Metallurgy A1-4 wt. % Ti and A1-6 wt. % Ti alloys have demonstrated potential for elevated temperature (200-300 C) aircraft applications. These materials derive their excellent strength, ductility, and creep resistance from their fine grain structure, oxide dispersion, and A1 Ti intermetallics. Inert gas atomization and mechanical alloying have been used to produce the binary alloy powders; however, Because of the large solidification range (1200-665 C) large quantities of primary $A1_3$ Ti were produced.

In this study, A1-Ti, A1-Ti-Ce, and A1-Ti-V alloy powders were produced by melt spinning. The alloys were fully characterized in order to assess the effect of composition and processing conditions on microstructure and phase stability. Optical and electron microscopy was used to study the morpohology and distribution of second phase disperoids. X-ray diffraction, differential scanning calorimetry (DSC), and selected area electron diffraction (SAD) techniques were used to establish the crystallography of the phases present.

The microstructure of the melt spun A1-Ti-X alloys have a higher volume fraction of finely dispersed submicron aluminides than did the previously studied inert gas atomized alloy powders. The major phases identified included A1 (fcc), $A1_3$ Ti (I4/mmm), and $A1_3$ Ti (I4/mmm).

20 DISTRIBUTION / AVAILABILITY OF ABSTRACT ☐ UNCLASSIFIED/UNLIMITED ☒ SAME AS RPT ☐ DTIC USERS	21 ABSTRACT SECURITY CLASSIFICATION Unclassified
22a NAME OF RESPONSIBLE INDIVIDUAL Dr. William E. Frazier	22b TELEPHONE (Include Area Code) 215-441-1301 22c OFFICE SYMBOL 6063

Introduction

Rapid Solidification Technology (RST)

Unique structures, morphologies, and metastable phases are associated with RST-produced alloys. The distinct microstructures observed are related to the alloy's response to rapid cooling from the melt. Freezing is necessarily associated with the heat of fusion; recalescence retards the rate at which the solid-liquid interface moves across the particle and tends to coarsen the previously solidified structure.(1,2) RST powders exhibit three distinct morphologies: microcrystalline, cellular, and dendritic.(3,4) The microcrystalline region is the most rapidly solidified structure which consists of an ordered arrangement of atoms and a uniform chemical composition. It is homogeneous, resists chemical attack, and is the slowest to coarsen. The cellular and dendritic microstructures correspond to slower cooling rates. Grant (5) has correlated cooling rate with secondary dendritic arm spacing (DAS) and powder size. Atomization results in cooling rates between 10^{3}-10^{5}K/s, DAS of 0.8-8.0 microns, and particle sizes of 20-250 microns in diameter; melt spinning produces cooling rates of 10^{5}-10^{7}K/s. The compositional gradients exist across the cellular and dendritic structures can serve as nucleation sites for possibly deleterious intermetallic compounds.

RST has been successful in producing alloys with mechanical properties which are substantially more resistant to thermal exposure than current wrought aluminum, e.g. 2219 (Al-6.3Cu-0.3Fe-0.2Si). In large part, the success stems from alloy additions of elements with high liquid state solubility, low solid state solubility and low solid state diffusion rates. High liquid solubility permits significant alloy additions. The low solid state solubility of the element in the matrix results in a high volume fraction of intermetallic compounds; the low diffusivity of the alloy addition decreases the rate of particle coarsening at service temperatures.

The current generation of elevated temperature RST aluminum alloys is based on transition elements, e.g., Al-Fe-X. Screening studies conducted by Sanders and Hildeman(6), Adams et al.(7) and Griffith et al.(8) have shown this composition to be an excellent compromise between ease of production and superior mechanical properties. The various materials producers have decided to pursue different ternary and quatanary compositions, e.g., Alcoa: Al-Fe-Ce, Alcan: Al-Cr-Zr, Allied: Al-Fe-V-Si, and Pratt and Whitney: Al-Fe-Mo.

Aluminum-Titanium System

Phase Equilibrium: The Al-Ti binary phase diagram is characteristic of alloys of widely differing melting points: Al-660°C., Ti-1660°C. There are several peritectic phase transformations and high melting point intermetallics, e.g., Al_3Ti. A peritectic phase transformation occurs at 665°C. and 1.15 wt.% Ti : Liquid + Al_3Ti transform to Al_3Ti. The exact wt.% Ti contained in the first solid to form during the peritectic decomposition is

reported to be between 1.15-1.3%.(9,10,11) At the transformation temperature, titanium solubility in the liquid is 0.12 wt.%.

Microstructure: The equilibrium phases present at room temperature are fcc aluminum and bct Al_3Ti. Numerous authors have investigated the solidification behavior of aluminum titanium alloys under near equilibrium conditions (12,13,14,15,). St.John(12) describes three types of Al_3Ti morphologies and classifies them as Type A, B, and C. The type A morphology is dendritic with all arms in one plane and mutually perpendicular. This structure was observed when the alloys were solidified under conditions of low temperature gradients or at low solidification rates and high temperature gradients. Type B particulates are described as "star-like" and/or "petal-like" in appearance. This morphology was found only in dilute alloys or under very high growth rate conditions. The Type C Al_3Ti particles are dendritic; primary, secondary, and tertiary arms growth occurs in a variety of directions but is confined to one crystallographic plane. Type C morphology was observed for alloys containing 3.5 to 5.0 wt.% Ti and at all solidification rates. Cisse´ et al.(15) studied the effect of solidification rate (1 to $100\ ^{o}Cs^{-1}$) on the morphology Al_3Ti. A plate-like structure was observed at slow cooling rates; however, as the solidification rate was increased, the Al_3Ti particles became progressively more petal-like in appearance.

Crystallography: The structure of aluminum is face centered cubic with a lattice parameter of 0.405 nm. Mondolofo (10) reports Al_3Ti has a body centered tetragonal (bct) structure, space group I4/mmm, 8 atoms/unit cell with a = 0.3851 nm and c = 0.86 nm.; density of 3.37 g/cm^3. In the precipitation of Al_3Ti from a supersaturated solid solution, an intermediate metastable coherent phase has been reported Al_3Ti'. This phase is believed to be similar to the cubic Al_3Zr' phase which has a space group Pm3m and 4 atoms/unit cell.(10) The Al_3Zr' forms as round particles changing to rods with a fan shaped pattern. The matrix-particle orientation is $(001)_p//(001)_{Al}$ $[100]_p//[100]_{Al}$.

Hashimoto et al.(16) and Kobayashi et al.(17) have studied the crystallography governing the nucleation of aluminum on Al_3Ti. The orientation relationships discovered can be classified into two categories: those involving semicoherent interfaces and those of the "so called" pseudo(near)-coincidence interface for which Coincidence-Site Lattice (CLS) analysis applies. The most consistent with the pseudo (near)-coincidence model is $(111)_{Al}//(112)_{Al3Ti}$, $[011]_{Al}//[110]_{Al3Ti}$. However, under relatively fast cooling conditions an orientation more consistent with the semicoherent interface model is frequently observed, i.e., $(001)_{Al}//(001)_{Al3Ti}$, $[100]_{Al}//[100]_{Al3Ti}$. Note, this is the same relationship previously described for the $Al-Al_3Zr$ interface.

Non-equilibrium Solidification: Metastable single phase aluminum can be obtained by rapidly cooling some Al-Ti alloys. The required cooling rate for partitionless solidification is a function of composition. Thus, for an alloy of 0.15 wt.% Ti, the required cooling rate is about $1\ ^{o}Cs^{-1}$ and for a 0.7 wt.%

Ti alloy, it is $150^{\circ}Cs^{-1}$.(18) Extrapolating data obtained from Kerr et al.(18) to cooling rates obtained during gas atomization, it is found that 1.4 wt.% Ti (3.5 vol.% Al_3Ti) could be trapped in solid solution. However, other workers have reported that rapid quenching from the liquid, up to 5 wt.% Ti can be held in solution.(10)

An interesting point is that with hyperperitectic alloys, increasing the cooling rate increases the nucleation temperature.(18,19) An approximation of the nucleation temperature and composition of the first solid to form can be obtained by extending the liquid-Al line upward into the Liquid-Al_3Ti phase region. Rapid solidification may suppress the formation of properitectic Al_3Ti, and hence, prevent the peritectic transformation.

Elevated Temperature Al-Ti-X Alloys

Titanium's low solid state solubility and low diffusivity in aluminum make Al-Ti-X alloys attractive for elevated temperature application. Initial attempts, however, to alloy aluminum with titanium proved unsuccessful.(7) Primarily because of the large temperature range over which these alloys solidify, conventional casting and gas atomization techniques produce microstructures consisting of coarse primary Al_3Ti platelets.

Recently, mechanical alloying and RST techniques have been used to produce Al-Ti-X alloys thermally stable to $300^{\circ}C$.(20,21,22) These alloys still contain unacceptable quantities of coarse, incoherent, primary intermetallic particles which degrade strength and toughness. This work examines the effect of rapid solidification and ternary alloying additions on particle size, morphology, and crystallography.

Experimental Procedure

Aluminum titanium alloys containing vanadium and cerium additions were prepared via melt spinning. This was done in order to assess the impact of rapid solidification and alloy composition on particle shape, morphology, and crystallography. The description of the experimental work is provided in two sections: (1) Materials Processing and (2) Microstructural Characterization. The materials processing section describes how the alloy powders were produced, consolidated, and extruded. The microstructural characterization section discusses how the structure and morphology of the powder alloys were evaluated.

Materials Processing

Powder Production: Seven different types of Al-Ti-X alloy ribbon, 2 Kg each, were produced by melt spinning at Marko Materials Inc.(Table I) Prior to consolidation, the ribbons were pulverized into 170-240 micron size particles.

Consolidation: The alloy powders were cold compacted at a pressure of 350 MPa into a 0.052m diameter 6061 aluminum can and vacuum degassed at 430°C for 1.5 hrs. The alloys were then extruded at 400°C and an extrusion ratio of 16.6:1 into 0.0127m diameter round rod.

Table I. Alloy Compositions, Wt.%

Alloy	Ti	V	Ce
1.	4	-	-
2.	3	-	3
3.	2	-	2
4.	2	-	1
5.	3	3	-
6.	2	2	-
7.	2	1	-

Microstructural Characterization

X-ray Diffraction: X-ray diffraction was utilized to identify the phases present in the powders and wrought alloys and establish the precise lattice parameters of the intermetallic phases. X-ray analysis was performed on a Rigaku DMAX B x-ray unit equipped with a theta/2-theta goniometer and a graphite monochromator. X-rays were generated using a copper tube operating at 50KV and 20ma. The scan rate was 1°/min and data was collected every 0.04 degrees.

Optical Microscopy: The alloy powders were mixed with fine ground dially phthalate powder and consolidated in a Buehler mounting press. The wrought alloys were mounted in a similar fashion. The mounted specimens were hand polished on successively finer grades of abrasive paper, i.e. 220, 320, 500, and 1000 grit. The samples were lapped using a 0.3 and a 0.05 micron alumina slurry. The specimens were observed in the etched(e.g., Keller's) and unetched condition on a Bausch and Lomb Research II metallograph.

Transmission Electron Microscopy (TEM): Thin foils of the materials were examined using a JEOL 100CX II transmission electron microscope operating at an accelerating voltage of 120kv. Samples were prepared for electropolishing by first using a jeweler's saw in order to cut the rod into 0.6mm thick sections. The specimens were hand ground to a thickness of 0.1mm and 3mm diameter disks were punched for electropolishing. Foils were prepared on a Struers twin jet electropolisher in a solution of 30% nitric acid and 70% methanol. The thinning conditions were 12v, 1.5ma, and a bath temperature of -30°C.

Alloy grain size and particle size determinations were made using TEM photographs taken at 50,000 times magnification. The mean grain and particle diameters were calculated by averaging feature length and feature breath.

Thermal Analysis: In order to assess the phase stability of the alloy rod, thermal analysis experiments were conducted using a DuPont 1090 thermal analyzer in conjunction with the differential scanning calorimeter (DSC) module. DSC heating curves were obtained at a heating rate of 10^{o}C/min using a pure aluminum sample as a reference material. A metered flow of dry helium gas kept the cell under a positive pressure.

Results and Discussion

Phase Identification and Crystallography

The x-ray diffraction scans for the Al-4Ti, Al-3Ti-3V, and Al-3Ti-3Ce alloy are presented in Figure 1. The phases found in the Al-4Ti alloy were fcc Al and bct Al_3Ti. The cerium containing alloy is composed of two or more phases: fcc aluminum, and perhaps Al_3Ti and orthorhombic alpha-Ce_3Al_{11}.

The vanadium bearing alloys are composed of two phases: fcc Al and a intermetallic compound, $Al_3(Ti_xV_{1-x})$, isostructural with bct Al_3Ti. Figure 2 is a plot of the lattice parameter, c, versus the fraction vanadium, 1-x, found in the intermetallic. The lattice parameter is seen to vary linearly with composition. The lattice parameter, a, behaves in a similar fashion. This enables one to tailor interplanar spacing by adjusting alloy composition.

X-ray diffraction profiles of the Al-3Ti-3Ce alloy ribbon before and after annealing at 600^{o}C for 24 hrs. are shown in Figure 3. Before annealing, the peaks are broad and of low intensity. However, after heat treatment the peaks gain intensity and definition. This behavior is also observed in the other alloys.

These results suggest two possibilities: (1) there is a increase in the size of the intermetallic particles, and (2) there is an increase in the volume fraction of intermetallics. The change in peak width (full width half height maximum) is known to be proportional to the wavelength of the x-ray source and inversely proportional to the cos(angle of the diffraction) times the particle diameter.(23) This relationship holds for particles less than 100nm in diameter. Therefore, it may be inferred that these alloys have a population of fine intermetallic particles (less than 100nm) which coarsen upon annealing.

Optical Microscopy

Optical micrographs of the etched alloy powders are presented in Figures 4. Microstructural variations can be observed through the ribbons' thickness. The intermetallic particles are seen as grey specks and increase in size and density. The ternary alloys also exhibit a featureless region resistant to chemical etching near the powders' surface.

The featureless "type A zones" have been observed in many rapidly solidified alloys and are described as microcrystalline or glass-like.(2) These featureless areas are the result of partitionless solidification. As solidification proceeds, the heat of fusion cause the velocity of the solid liquid interface to slow, thus, permitting solute partitioning. The net effect is a microstructural variation through the melt spun ribbon's thickness.

In the microstructures of the alloy rods, prior particle boundaries (PPB) are clearly visible as dark grey grain boundaries elongated along the extrusion direction. The plate-like second phase intermetallic particles are non-uniformly distributed and preferentially aligned in the extrusion direction.

Transmission Electron Microscopy (TEM)

TEM was used to examine the microstructures of the alloy rods. Representative photomicrographs are presented in Figure 5. Results of the quantitative microstructural evaluation, of alloys' grain and particle sizes, are presented in Table II.

The microstructural appearance of alloys Al-4Ti and Al-3Ti-3V are similar, Figures 5a & 5c. Grain boundary triple points are pinned by spherical and cuboidal intermetallic particles. Elongated particles lie preferentially along grain boundaries and fine spherical particles are interdispersed throughout the grain interior.

Table II. Microstructural Dimensions, microns

ALLOY	GRAIN SIZE	PARTICLE DIAMETER
Al-4Ti	0.9	0.17
Al-3Ti-3Ce	0.7	0.14
AL-3Ti-3V	1.1	0.21

The microstructure of the Al-3Ti-3Ce is less uniform than the Al-4Ti and Al-3Ti-3V alloys, i.e., grain and particle sizes vary greatly within the same specimen. In addition, there are areas in the material which appear devoid of dispersoids. The larger particles, 1 to 2 microns in diameter, have the appearance of being aggregates of the fine, 0.5 micron diameter, particles.

Thermal Analysis

Differential scanning calorimetry thermograms of the alloys are flat to 400°C. This suggests that no phase transformations, e.g., precipitation, recrystallization, grain growth, etc., are occurring below 400°C.

A broad, poorly defined, exothermic reaction peak is observed in the alloys above 400°C. This weak exothermic peak (4-10 J/g) is probably associated with a low energy phase transformation such as Ostwald ripening or grain growth. It is interesting to note that this is the temperature regime in which the materials were degassed and extruded. The DSC results suggest that the thermomechanical processing history of these alloys serves to stabilize their microstructures below 400°C.

Conclusions

Al_3Ti and Al_3V are isostructural (4I/mmm); vanadium substitutes freely for titanium permitting the formation of an $Al_3(Ti_x, V_{1-x})$ intermetallic compound. Thus, the lattice parameters of this intermetallic falls between that of Al_3Ti and Al_3V.

The faster solidification rates associated with melt spinning in comparison to inert gas atomization effect a reduction in the size and quantity of the primary intermetallic phase.

The resistance of the alloy powders to chemical etching varies across the thickness of the powder particles. The size of the intermetallic particles become greater as the distance from the wheel-metal interface increases.

DSC thermograms of the alloys indicate that the alloys are stable below 400°C.

References

1. C.G. Levi and R. Mehrabian, "Heat Flow During Rapid Solidification of Undercooled Metal Droplets," Metallurgical Transactions A., 13A (1982) p.221.
2. H. Jones, "Observations on a Structural Transition in Aluminum Alloys Hardened by Rapid Solidification," Material Science and Engineering, 5 (1969).
3. J.R. Manning, J.G. Early, W.B. Boettinger, L.A. Bendersky, and F.S. Biancaniello, 1st Quarterly Report, "Consolidation of Rapidly-Solidified High Temperature Aluminum Alloys," (Contract No. N000198WR41136, NBS, June, 1984).

4. J.R. Manning, J.F. Early, W.J. Boettinger, L.A. Bendersky, and F.S. Biancaniello, Second Quarterly Report, "Consolidation of Rapidly-Solidified High Temperature Aluminum Alloys," (Contract No. N62269-84WR-00198, NBS, Oct., 1984).
5. N. Grant, "Rapid Solidification of Metallic Particles," High Strength Powder Metallurgy Aluminum Alloys, ed. M.J. Koczak and G.J. Hildeman (Warrendale, PA: TMS, 1982), p.3.
6. R.E. Sanders, Jr., and G.H. Hildeman, "Elevated Temperature Aluminum Alloy Development," Final Report, (Contract No. F-3315-77-C-5086, AFWAL, 1981).
7. C.M. Adam, R.G. Bourdeau, J.W. Broch, and A.R. Cox, "Application of Rapidly Solidified Alloys," Final Report, (Contract No. F-33615-76-C-5136, AFWAL, 1981).
8. W.M. Griffith, R.E. Sanders, Jr., and G.J. Hildeman, "Elevated Temperature Aluminum Alloys for Aerospace Applications," High Strength Powder Metallurgy Aluminum Alloys, ed. M.J. Koczak and G.J. Hildeman (Warrendale, PA: TMS, 1982), p.209.
9. D.H. St. John and L.M. Hogan, "Thermal Stability in the Al-Al_3Ti System," Journal of Material Science, 15 (1980) p.2369.
10. L.F. Mondolfo, Aluminum alloys: Structure and Properties. (London-Boston: Butterworths, 1979).
11. M. Hansen, Constitution of Binary Alloys. (New York: McGraw-hill, 1958).
12. D.H. St. John, and L.M. Hogan, "Metallography and Growth Crystallography of Al_3Ti in Al-Ti Alloys up to 5 wt.% Ti," Journal of Crystal Growth, 46 (1979) 387-398.
13. D.H. St. John, and L.M. Hogan, "Segregation Patterns in Unidirectionally Solidified Al-Ti Solid Solution Alloys," Journal of Crystal Growth, 46 (1979) 585-587.
14. H. El-Halfawy et al., "Al_3Ti Precipitates in a Chill-Cast Al-14 wt.% Ti Alloy," Metallography, 12 (9) (1979).
15. J. Cisse, H.W. Kerr, and G.F. Bolling, "The Nucleation and Solidification of Al-Ti Alloys," Metallurgical Transactions, 5 (1974) p.633.
16. S. Hashimoto, K.F. Kobayaski, and S. Miura, "Roles of Lattice Coherency to the Heterogeneous Nucleation in the Al-Ti System," Zeitschifl Fuer Metallkunke, (Dec., 1983).
17. J.W. Martin and R.D. Doherty, Stability of Microstructure in Metallic Systems (Cambridge: Cambridge Univ. Press, 1980).
18. H.W. Kerr, J. Cisse, and G.F. Bolling, "On Equilibrium and Non-Equilibrium Peritectic Transformations," Acta Metallurgica, 22 (1974) p.677.
19. D.H. St. John and L.M. Hogan, "The Peritectic Transformation," Acta Metallurgica, 25 (1977) p.77.
20. H.G.F. Wilsdorf et al., "Very High Temperature Aluminum Materials Concepts," Biannual report No. 2, (AFWAL Contract No. F33615-86-C-5074, University of Virginia, 1987).
21. W.E. Frazier, "A Fundamental Study of the Mechanical and Microstructural Response of Elevated Temperature PM Aluminum-Titanium Alloys," (Ph.D. thesis, Drexel University, 1987).

22. G.S. Murty, M.J. Koczak, and W.E. Frazier, "High Temperature Deformation of Rapidly Solidified Processed/Mechanically Alloyed Al-Ti Alloys," Scripta Metallurgica, 21 (2)(1987) 141-146
23. B.D. Cullity, Elements of X-ray Diffraction. (Reading, Massachusetts: Addison-Wesley, 1978), 284.

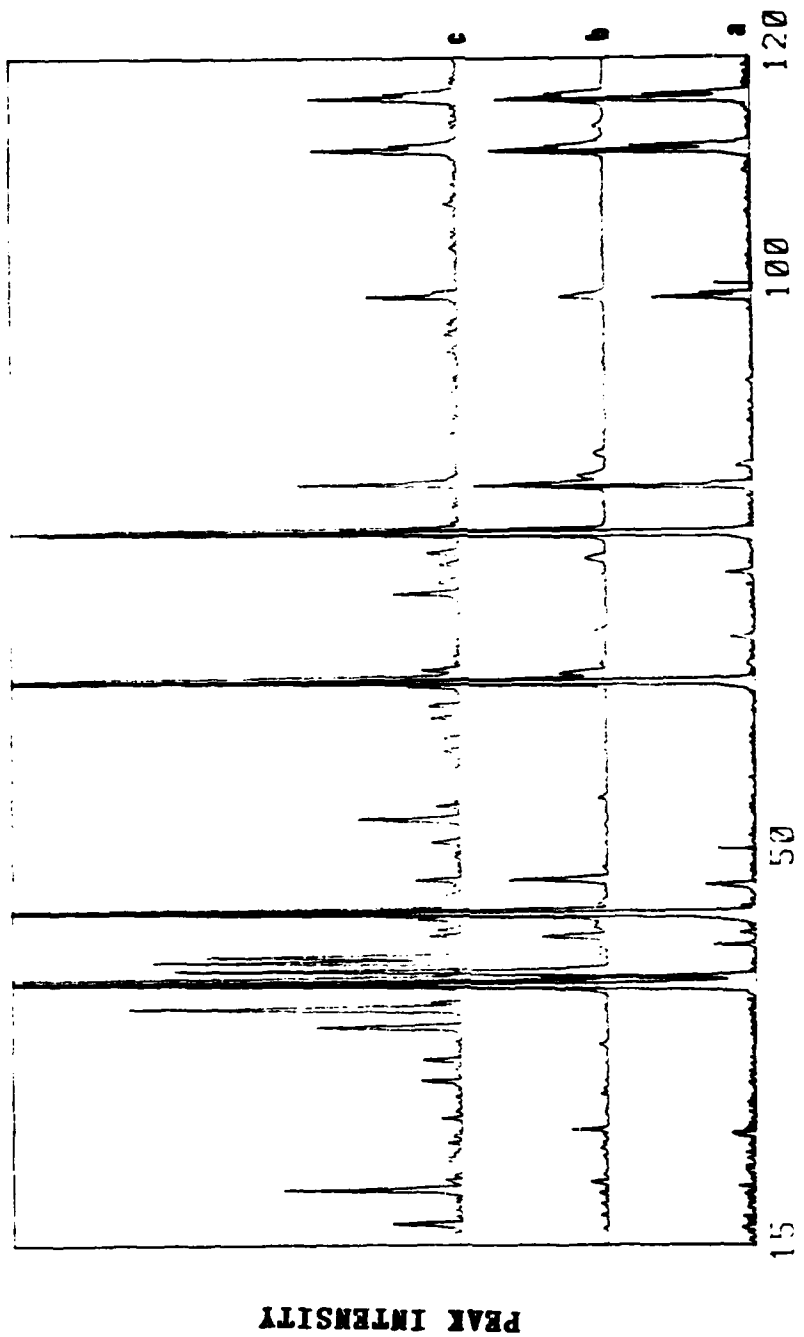

Figure 1. X-ray Diffraction Profiles of Annealed Alloy Ribbon: (a) Al-4Ti, (b) Al-3Ti-3V, and (c) Al-3Ti-3Ce.

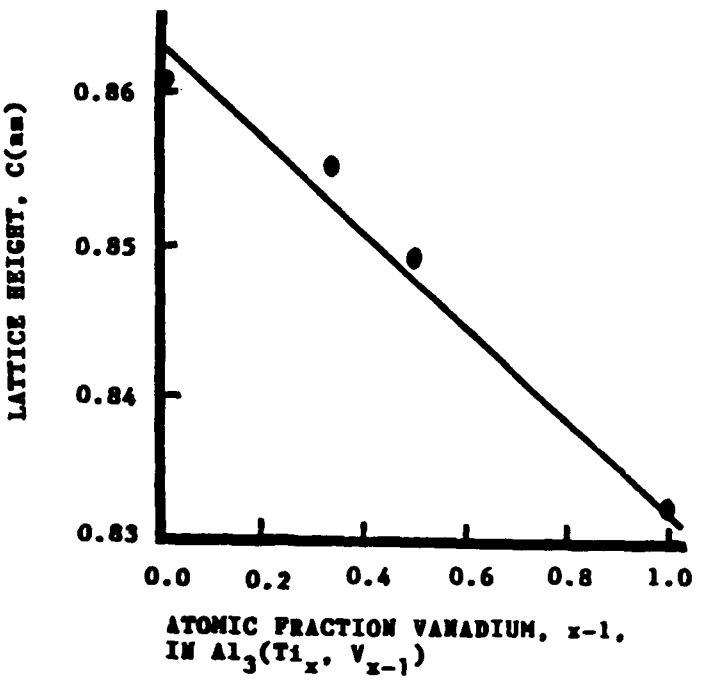

Figure 2. The Effect of Vanadium Content on the Lattice Parameter, c, of $Al_3(Ti, V)$

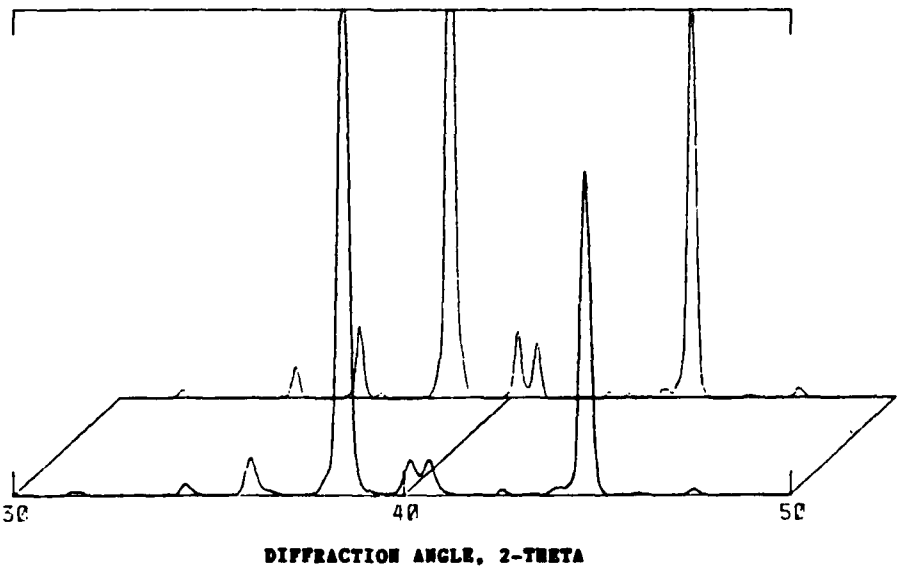

Figure 3. X-ray Diffraction Profiles of Al-3Ti-3Ce Ribbon: (a) As-received, and (b) Annealed at 600°C for 24 Hours.

(a)

(b)

(c)

Figure 4. Optical Micrographs of the Alloy Powders: (a) Al-4Ti, (b) Al-3Ti-3Ce, and (c) Al-3Ti-3V.

(a)

(b)

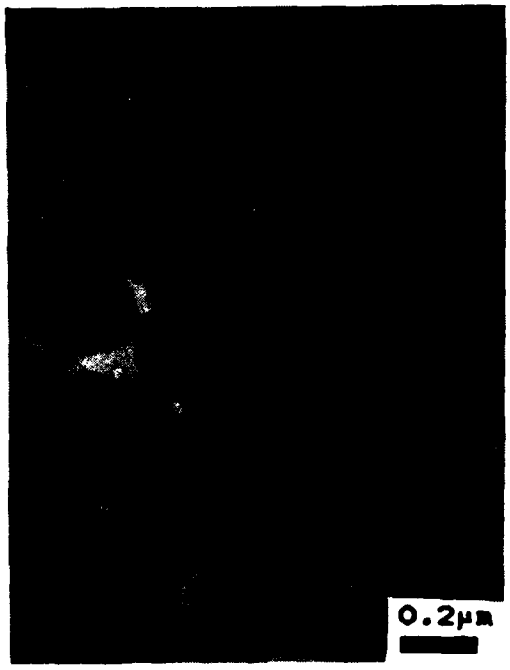

(c)

Figure 6. TEM Micrographs of the Alloy Powders: (a) Al-4Ti, (b) Al-3Ti-3Ce, and (c) Al-3Ti-3V.

United Technologies, Pratt and Whitney, P.O. Box 2691,
West Palm Beach, Fl. 33402, J. Simon Jr. 1
USAF Systems Command, WPAFB, OH 45331 1
University of Calfornia, Dept. of Mechanical Engineering, Irvine, CA
92717, E.J. Lavernia 1
University of Virgina, Light Metals Center, Charlottesville,
VA 22901, J. Wert, J. Hawk, E.A Starke, Jr. 3

McDonnell Aircraft Co., Box 516, Saint Louis, MO 63166, V.M. Vasey-Glandon and K.K. Sankaran 2
MCIC, Battelle Memorial Institute, Columbus OH 1
Metcut-Materials Research Group, P.O. Box 33511, Wright Patterson AFB, OH 45433, Y.W. Kim 1
NASA Headquarters, 600 Independence Av., Washington, DC 20546, Mr. N. Mayer 1
NASA Langley Research Center, Hampton, VA 23365, A. Taylor 1
National Bureau of Standards, Gaithersburg, MD 20899, J.R. Manning 1
NAVAIRDEVCEN, Warminster, PA, 18974-5000, Library, Code 8131 (3 Copies), W.E. Frazier, Code 6063 (27 Copies) 30
0
NAVAVNDEP, MCAS, Cherry Point, CA Code 340 1
NAVAVNDEP, NAS, Alameda, CA Code 340 1
NAVAVNDEP, NAS, Jacksonvelle, FL Code 340 1
NAVAVNDEP, NAS, Norfolk VA Code 340 1
NAVAVNDEP, NAS, North Island, CA Code 340 1
NAVAVNDEP, NAS, Pensacola, FL Code 340 1
NAVAIRSYSCOM, Washington, DC 20361, J. Collins Air-5304, L. Sloter Air 931 2
NAVAIRTESCEN, Patuxent River, MD 1
Naval Air Propulsion Test Center, Trenton, NJ 08628, R. Mahortor 1
Naval Surface Weapons Center, Dahlgren, VA 22448-5000, 1
Naval Surface Weapons Center, Silver Spring, MD 20903-5000, D. Divecha 1
Naval Post Graduate School, Mechanical Engineering Department, Monterey, CA 93943, 1
Naval Research Laboratory, Washington, DC 20375, Code 6120, Code 6306 2
Naval Ship Engineering Center, Washington DC 20360, Code 6101E, 1
NAVAVNSAFECEN, NAS Norfolk VA, 1
NAVSEASYSCOM, Washington, DC 20362 1
NAVSHIPRANDCEN, Annapolis, MD 21402 1
NAVSHIPRANDCEN, Bethseda, MD 20034 1
Northrop, Aircraft Division, One Northrop Av., Hawthorne, CA 90250, S.P. Agrawal and G.R. Chanani 2
National Science Foundation, Office of Science and Technology Centers Division, 1800 G Street, Washington, DC 20550 1
Office of Naval Research, Washington, DC 20350, S. Fishman Code 431 1
Office of Naval Technology, Arlington, VA, J. Kelley OCNR-225 1
Reynolds Metals Co., Fourth and Canal St., P.O. Box 27003, D. Thompson 1
Rockwell International, Science Center, 1049 Camino Dos Rios, P.O. Box 1085, Thousand Oaks, CA 91360 1
Sandia National Laboratory, Alburquerque, NM 87185, Div. 1822 and 1832 2
TRW, Inc., 23555 Euclid Av., Cleveland, OH 44117 1
U.S. Army Air Mobility R&D Laboratory, Fort Eustis, VA 23064, SAVDL-EU-SS 1

Distribution List

	No.
Air Force Wright Aeronautical Lab.,Wrigth Patterson AFB, OH 45433, W. Griffith	1
Alcan Rolled Products Co., 100 Erieview Plaza, Cleveland, OH 44114, P. Wakeling	1
Alcoa, 1501 Alcoa Building, Pittsburg, PA 15219, F.R. Billman and G.J. Hildeman	2
Allied Corp., P.O. Box 1021R, Morristown, NJ 07960, S.K. Das and P. Gilman	2
Army Materials and Mechanics Research Center, Watertown, MA	1
Avco Corp., Applied Technology Divison, Lowell, MA 01851	1
Battelle Memorial Institute, Columbus Laboratories, 505 King Av., Columbus, OH 43201	1
Boeing Commercial Airplane, Seatle WA , W. Quist	1
Boeing Corp., Aerospace Division, P.O. Box 3707, Seatle, WA 98124	1
Boeing-Vertol Co., P.O. Box 16858, Phila., PA 19142, Dept. 1951	1
British Alcan Aluminum Ltd., Alcan International, Southam Rd., Bambury, Orfordshire OX 167SP, United Kingdom, R. Grines	1
Brookhaven National Laboratory, Department of Applied Science/PSD, Building 526, Upton, NY 11973	1
Clemson University, Dept. of Mechanical Engineering, Riggs Hall, Clemson, SC 29634-0921, H.J. Rack	1
DARPA, 1400 Wilson Blvd., Arlington, VA 22209, B. Wilcox	1
Defense Technical Information Center, Cameron Station, Bldg. 5, Alexandria, VA 22314	1
Department of Energy, 100 Independence Av., SW Washington, DC 20585, Code CE142	1
Drexel University, Dept. of Materials Engineering, 32nd and Chestnut St., Phila., PA 19104, M.J. Koczak	1
General Dynamics, Convair Aerospace Division, P.O. Box 748, Fort Wort, TX 76101, Tech. Library	1
General Electric Co., Valley Forge Space Center, Phila., PA 19101	1
Grumman Areospace Corp., Bethpage, NY 11714, P.N. Adler	1
Inco Alloys International, P.O. Box 1958, Huntington, WV 25720, R. Schelleng and R. Benn	2
Innovare Inc., Ben Franklin Technology Center, South Mountain Dr., Bethlehem, PA 18015, A.R. Austen	1
Kaiser Aluminum, Ravenswood works, Ravenwood, WV 26164, J. M. Hunter	1
Lockheed California Co., Burbank, Ca 91520-7631, D.J. Chellman	1
Lockheed Missiles and Space Co., Metallurgy Dept. 93-10/204, 3251 Hanover St., Palo Alto CA 94304, R. Lewis and J. Wadworth	2
Marko Materials Inc., 144 Rangeway Rd., N. Billerica, MA 01862, R. Ray	1
Martin Marietta Laboratories, 1450 South Rolling Rd., Baltimore, MD 21227-3898, J. Venables	1
Material Science Corporation, 1777 Walton Rd., Blue Bell, PA 19422	1